

**Marquette University**  
**e-Publications@Marquette**

---

Civil and Environmental Engineering Faculty  
Research and Publications

Civil and Environmental Engineering, Department  
of

---

1-1-2017

# Autocatalytic Pyrolysis of Wastewater Biosolids for Product Upgrading

Zhongzhe Liu

*Marquette University*, [zhongzhe.liu@marquette.edu](mailto:zhongzhe.liu@marquette.edu)

Patrick J. McNamara

*Marquette University*, [patrick.mcnamara@marquette.edu](mailto:patrick.mcnamara@marquette.edu)

Daniel Zitomer

*Marquette University*, [daniel.zitomer@marquette.edu](mailto:daniel.zitomer@marquette.edu)

---

Accepted version. *Environmental Science & Technology*, Vol. 51, No. 17 (2017): 9808-9816. DOI. © 2017 American Chemical Society. Used with permission.

Marquette University

**e-Publications@Marquette**

***Civil and Environmental Engineering Faculty Research and Publications/College of Engineering***

***This paper is NOT THE PUBLISHED VERSION; but the author's final, peer-reviewed manuscript. The published version may be accessed by following the link in the citation below.***

*Environmental Science & Technology*, Vol. 51, No. 17 (2017): 9808-9816. [DOI](#). This article is © American Chemical Society and permission has been granted for this version to appear in [e-Publications@Marquette](#). American Chemical Society does not grant permission for this article to be further copied/distributed or hosted elsewhere without the express permission from American Chemical Society.

**Autocatalytic Pyrolysis of Wastewater Biosolids for Product Upgrading**

Zhongzhe Liu

Department of Civil, Construction and Environmental Engineering, Marquette University, Milwaukee, WI

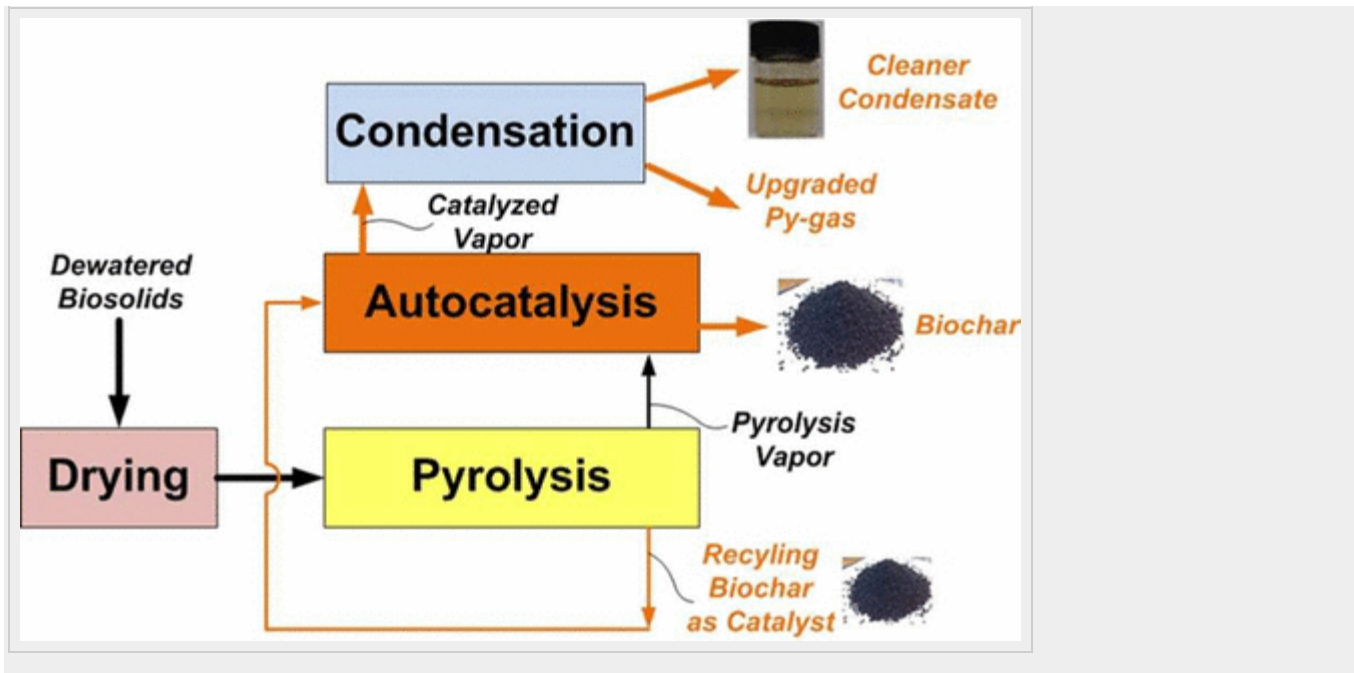
Patrick McNamara

Department of Civil, Construction and Environmental Engineering, Marquette University, Milwaukee, WI

Daniel Zitomer

Department of Civil, Construction and Environmental Engineering, Marquette University, Milwaukee, WI

## Abstract



The main goals for sustainable water resource recovery include maximizing energy generation, minimizing adverse environmental impacts, and recovering beneficial resources. Wastewater biosolids pyrolysis is a promising technology that could help facilities reach these goals because it produces biochar that is a valuable soil amendment as well as bio-oil and pyrolysis gas (py-gas) that can be used for energy. The raw bio-oil, however, is corrosive; therefore, employing it as fuel is challenging using standard equipment. A novel pyrolysis process using wastewater biosolids-derived biochar (WB-biochar) as a catalyst was investigated to decrease bio-oil and increase py-gas yield for easier energy recovery. WB-biochar catalyst increased the py-gas yield nearly 2-fold, while decreasing bio-oil production. The catalyzed bio-oil also contained fewer constituents based on GC-MS and GC-FID analyses. The energy shifted from bio-oil to py-gas, indicating the potential for easier on-site energy recovery using the relatively clean py-gas. The metals contained in wastewater biosolids played an important role in upgrading pyrolysis products. The Ca and Fe in WB-biochar reduced bio-oil yield and increased py-gas yield. The py-gas energy increase may be especially useful at water resource recovery facilities that already combust anaerobic digester biogas for energy since it may be possible to blend biogas and py-gas for combined use.

## Introduction

Water resource recovery facilities (WRRFs) face multiple challenges at the nexus of energy generation, nutrient recovery, and pollutant removal.<sup>1-4</sup> Improving onsite energy generation and recovering value-added products are common goals for sustainable water resource reclamation. In addition, removing micropollutants is important for water reuse applications and public health.

Wastewater biosolids are a major byproduct from WRRFs, and over eight million dry tons are produced annually in the United States, of which over 55% are land applied because of their beneficial soil conditioner properties.<sup>5</sup> Even though biosolids are stabilized using processes such as anaerobic digestion, residual energy in refractory biosolids is not recovered before biosolids land application.<sup>6</sup> In addition, micropollutants such as organic contaminants of emerging concern and pathogens in biosolids are also public health issues.<sup>7-11</sup> For instance, biosolids land application is banned in some jurisdictions such as Switzerland due to perceived environmental issues regarding emerging contaminants.<sup>12,13</sup> Therefore, post-treatment techniques to maximize energy recovery, minimize adverse environmental impacts, and reduce public health concerns due to biosolids reuse are critical elements for sustainable resource recovery.

In addition to anaerobic digestion, other biosolids handling technologies are employed or are under development for energy and resource recovery, including incineration, gasification, and pyrolysis.<sup>14-18</sup> Sludge incineration is an established process for energy production; however, it does not yield a high-quality soil-amendment product, and nutrients in biosolids are wasted in ash that is typically disposed of in landfills. Also, sludge incineration has air emission concerns including the possibility of heavy metals and organic chemicals in flue gas.<sup>19,20</sup> Sludge gasification (i.e., converting sludge at high temperature of over 700 °C using a substoichiometric amount of oxygen and/or steam) produces synthesis gas that can be used for energy production or converted to liquid fuel or chemicals,<sup>16,21</sup> but the solid product is ash-rich char with little or no agricultural value.

Pyrolysis is a thermochemical process that decomposes organic matter upon heating at elevated temperatures under anoxic conditions. Compared to other thermochemical processing techniques, biosolids pyrolysis can be more favorable in terms of energy recovery, resource recovery, and contaminant removal. A recent study concluded that biosolids pyrolysis could be a low-waste solution to biosolids handling in Europe when compared to incineration and gasification.<sup>22</sup> Biosolids pyrolysis produces biochar, a valuable soil amendment that results in improved soil moisture-holding capacity and plant growth, along with pyrolysis gas (py-gas) and bio-oil that can both be used as fuel.<sup>17</sup> Previous research demonstrated that biochar can be used to sorb nutrients from digested wastewater sludge filtrate generated by belt filter presses. When added to soil, the biochar with sorbed nutrients resulted in a grass growth rate similar to that of commercial fertilizer.<sup>23</sup> Furthermore, biosolids pyrolysis removes micropollutants such as triclosan and triclocarban as well as reduces total estrogenicity of the solid material produced.<sup>24,25</sup> It may be beneficial to couple existing solids drying systems in WRRFs to pyrolysis. Biosolids drying is the most energy intensive portion of the pyrolysis process, and py-gas can be used to provide heat for drying.<sup>26</sup>

Most biosolids pyrolysis studies have focused on slow pyrolysis (hereafter referred to as pyrolysis). The yields and properties of the three pyrolysis products have been characterized using different temperature, residence time, heating rate, and feedstock types.<sup>27-36</sup> Crude biosolids-derived bio-oil (i.e., pyrolysis condensate, hereafter referred to as bio-oil) normally accounts for approximately 40%

(by mass) of the total biosolids pyrolysis products.<sup>18,32</sup> This bio-oil often contains a light nonaqueous phase as well as an aqueous phase containing water and soluble organics. However, unlike py-gas, which can be used directly in traditional power generator systems such as those employing internal combustion engines,<sup>37</sup> direct combustion of bio-oil alone requires costly pretreatment as well as modification of combustion systems and operating conditions due to its high viscosity, acidity, water content, and corrosiveness.<sup>38,39</sup> In addition, the bio-oil aqueous phase has no apparent use and must be managed. Alternatively, light nonaqueous bio-oil phase can be upgraded using hydrogen and catalysts to produce drop-in-grade fuels such as diesel, but these technologies are still under development.<sup>40</sup> Fonts et al. concluded that full-scale implementation of biosolids pyrolysis has been limited by the low economic value of the bio-oil product.<sup>34</sup> Since py-gas is relatively clean and can be easily burned in gas engines and boilers, reducing bio-oil yield and increasing cleaner py-gas yield is a promising approach to intensify on-site energy recovery at WRRFs.

Catalysis could be an efficient means to reduce bio-oil production while increasing py-gas yields. Typical bio-oil is largely composed of primary tars,<sup>41</sup> a black mixture of high molecular weight hydrocarbons such as aromatics.<sup>42</sup> The destruction of tar using certain chars as catalysts has proven to be effective.<sup>43-49</sup> In particular, biochar derived from wood and corn stover were used as catalysts to increase py-gas yield.<sup>44,50,51</sup> Research on the catalytic effect of wastewater biosolids-derived biochar (WB-biochar) during wastewater biosolids pyrolysis is lacking. The objective of this research was to determine the autocatalytic potential of WB-biochar on the yield and compositions of py-gas and bio-oil. Also, mechanistic experiments were conducted to determine why WB-biochar was an effective catalyst.

## Methodology

### Biosolids Autocatalytic Pyrolysis

A laboratory system ([Figure 1](#)) was used to pyrolyze dried biosolids (Milorganite) from a WRRF (Jones Island Water Resource Recovery Facility, Milwaukee, Wisconsin). Dried biosolids was a blend of waste activate sludge and anaerobically digested primary solids with volatile solids, fixed carbon, and ash content values of 66.6%, 7.70%, and 25.7%, respectively (wt %, dry basis) using the ASTM D7582 standard.<sup>52</sup> Dried biosolids contained 36.5% carbon, 4.62% hydrogen, 7.18% nitrogen, 1.09% sulfur, and 24.89% oxygen (oxygen calculated by difference on a dry basis) (Vario Micro Cube, Elementar, Hanau, Germany).

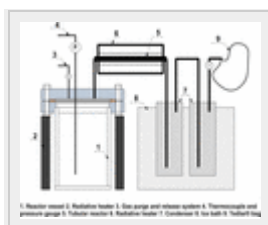


Figure 1. Schematic of lab-scale pyrolysis system.

The pyrolytic system consisted of a stainless-steel reactor vessel (360 cm<sup>3</sup>, 7.1 cm inner diameter, 8.9 cm long), a ceramic radiative heater, a gas purge and release system, a stainless-steel tubular reactor (0.79 cm inner diameter, 27.9 cm long), an ice bath for liquid condensation, and a gas collection system coupled to a Tedlar bag. Pressure and temperature at different locations were monitored by pressure gauges and thermocouples, respectively. Batch reactors were used for lab-scale study, but other configurations such as screw-conveyor or rotary kiln reactors may be used in full-scale applications.

Dried biosolid particles that were sieved to 1–2 mm nominal diameter were pyrolyzed by purging the pyrolysis vessel with argon gas at 15 mL/min. Catalyst particle size of 0.5–1 and 1–2 mm were compared during preliminary testing, and no obvious differences in catalytic effects were observed. The heating rate was controlled from 8 to 15 °C/min, and the retention time of each test was 30 min after the reactor reached the desired pyrolysis temperature. Argon flow was shut off when the retention time was over. Pyrolysis vapor passed through stainless tubing to condensers in an ice bath in which bio-oil and py-gas were separated. Py-gas was collected in a Tedlar bag. The masses of biochar and bio-oil were measured gravimetrically. Coke (i.e., carbon-rich solid material produced by carbonization of high-boiling hydrocarbons) can be formed on the biochar catalyst in the tubular reactor due to decomposition of heavy hydrocarbons.<sup>53</sup> The coke mass yield was determined by measuring the weight gain of the spent biochar catalyst. The py-gas mass was calculated by difference (i.e., initial biosolids mass minus the sum of biochar, bio-oil, and coke masses).

For autocatalytic pyrolysis (i.e., pyrolysis whereby a product (biochar) is used in the process itself as a catalyst), the tubular reactor was filled with WB-biochar catalyst and preheated to the desired temperature. The catalyst was produced from 500 to 800 °C using the aforementioned pyrolysis method. The autocatalytic performance was evaluated by varying pyrolysis temperature (500–800 °C) and catalyst/biosolids mass ratio (0.2–1). The temperature used to generate the biochar was identical to the experimental pyrolysis temperature (i.e., biochar made at 800 °C was used for 800 °C autocatalytic pyrolysis experiments). All pyrolysis experiments were performed in triplicate.

#### Biosolids Noncatalytic Pyrolysis

Two noncatalytic pyrolysis tests were also performed as controls. For the first noncatalytic test (OS test), inert sand with nominal particle diameter from 1 to 2 mm was added to the tubular reactor in place of WB-biochar catalyst to observe any effect of secondary, homogeneous reactions among vapor components at high temperature.<sup>44,50</sup> The packed sand and WB-biochar catalyst had similar porosities of 46% and 50%, respectively, indicating similar residence times for the pyrolysis vapor in the tubular reactor. The porosities were determined by a water saturation method.<sup>54</sup> For the second noncatalytic test (OB), an empty tubular reactor was maintained at 500 °C to achieve conventional bio-oil condensation with a minimized secondary, homogeneous reactions. The tubular reactor was kept at 500 °C to prevent pyrolysis vapor constituents from condensing during conveyance downstream. The detailed experimental designs of noncatalytic and autocatalytic testing are listed in [Table 1](#).

**Table 1. Experimental Design of Autocatalytic, Noncatalytic, and Mechanistic Tests**

	Reactor Temperature (°C)	Downstream Temperature (°C)	Downstream Loading	Catalyst/Biosolids Mass Ratio
Autocatalytic	500	500	1–2 mm biochar	0.2, 0.33, 1
	600	600	1–2 mm biochar	0.2, 0.33, 1
	700	700	1–2 mm biochar	0.2, 0.33, 0.5, 1
	800	800	1–2 mm biochar	0.2, 0.33, 0.5, 1
Noncatalytic (0S)	500	500	1–2 mm sand	0
	600	600	1–2 mm sand	0
	700	700	1–2 mm sand	0
	800	800	1–2 mm sand	0
Noncatalytic (0B)	500	500	Blank	0
	600	500	Blank	0
	700	500	Blank	0
	800	500	Blank	0
Mechanistic (Bio-oil decomposition and reforming)	800	800	1–2 mm biochar	Catalyst/Bio-oil mass ratio: 1:1.08 (similar to catalyst/biosolids mass ratio of 0.33)
Mechanistic (Simulated py-gas reforming)	800	800	1–2 mm biochar	Flow rate: 200 mL/min (similar to catalyst/biosolids mass ratio of 0.33)

	Reactor Temperature (°C)	Downstream Temperature (°C)	Downstream Loading	Catalyst/Biosolids Mass Ratio
Mechanistic (Simulated catalysts)	800	800	MgCl <sub>2</sub> , CaCl <sub>2</sub> , FeCl <sub>3</sub> , MgO, CaO, Fe <sub>2</sub> O <sub>3</sub> impregnated DDGS-biochar	0.33

#### Mechanistic Studies Using Bio-Oil or Simulated Py-Gas Alone

The autocatalytic effects of WB-biochar on both bio-oil and py-gas alone were investigated using a bio-oil decomposition and reforming test as well as a py-gas reforming test, respectively. For the bio-oil decomposition and reforming test, the noncatalytic bio-oil (produced using OB conditions at 800 °C) was placed in the reactor vessel, and WB-biochar catalyst was placed in the tubular reactor. The catalyst/bio-oil mass ratio was 1:1.08. This ratio was similar to that observed when pyrolyzing biosolids at a catalyst/biosolids mass ratio of 0.33. The reactor vessel and tubular reactor temperatures were 800 °C. Catalyzed bio-oil and py-gas products and coke were measured according to the procedures for biosolids pyrolysis described above.

For py-gas reforming tests, a simulated noncatalytic py-gas (i.e., a gas with similar composition to py-gas from OB at 800 °C) containing the following components was used: 10% CH<sub>4</sub>, 27.5% CO, 31.5% H<sub>2</sub>, 27.5% CO<sub>2</sub> (Airgas, West Allis, Wisconsin). This simulated py-gas was fed to the pyrolysis system at a flow rate of 200 mL/min. This flow rate was similar to flow rates observed during biosolids pyrolysis experiments. The simulated py-gas was heated in the 800 °C empty reactor vessel before entering the 800 °C tubular reactor filled with WB-biochar. Reformed gas exiting the tubular reactor was collected in a Tedlar bag for gas composition analysis.

#### Autocatalytic Role of Dominant Metals in WB-Biochar

WB-biochar contains a high concentration of metals such as Mg, Fe, and Ca. These metals could have catalytic potential to upgrade bio-oil by destroying high molecular weight hydrocarbons (e.g., tar).<sup>55-60</sup> Based on elemental analysis by X-ray fluorescence (XRF-1800, Shimadzu), Mg, Ca, and Fe were present in the WB-biochar that was used in this study ([Table S1](#)). It was hypothesized that these metals improved autocatalytic pyrolysis. Therefore, simulated biosolids biochar catalysts were produced to investigate the catalytic influence of metals. The simulated biosolids biochar catalysts were made by impregnating biochar produced from dried distillers grains with solubles (DDGS) with various metals. DDGS was employed because the resulting biochar surface area was similar to that of WB-biochar, but DDGS biochar had low metals content ([Table S1](#)) and also demonstrated minimal catalytic activity when exposed to biosolids pyrolysis vapor ([Figure S1](#)).

Six simulated biosolids biochar catalysts were prepared using Mg<sup>2+</sup>, MgO, Ca<sup>2+</sup>, CaO, Fe<sup>3+</sup>, or Fe<sub>2</sub>O<sub>3</sub> to obtain various metal concentrations (nominally 3% Mg, 7% Ca, and 11% Fe) in biochar. MgCl<sub>2</sub>, CaCl<sub>2</sub>,



and FeCl<sub>3</sub> were selected as the salt precursors. Mg(NO<sub>3</sub>)<sub>2</sub>, Ca(NO<sub>3</sub>)<sub>2</sub>, and Fe(NO<sub>3</sub>)<sub>3</sub> were selected as the oxide precursors. Each precursor was dissolved in deionized water and mixed with DDGS biochar. The mixture was dried and then activated by calcination at 500 °C for 3 h in an oxygen-free environment. The actual metal concentrations in the simulated biochar catalysts were confirmed by acid digestion to be 2.8% Mg, 6.7% Ca, and 10.7% Fe by dry weight. All mechanistic experiments were performed in triplicate at 800 °C with a catalyst/biosolids mass ratio of 0.33 since this ratio yielded observable increases in py-gas at 800 °C, but higher catalyst/biosolids ratios did not substantially increase py-gas yields ([Table 1](#)). Statistical analyses (*t* test,  $\alpha$  level = 5%) were performed using Microsoft Excel.

### Product Analyses

Py-gas composition (H<sub>2</sub>, CH<sub>4</sub>, CO, C<sub>2</sub>H<sub>4</sub>, C<sub>2</sub>H<sub>6</sub>, CO<sub>2</sub>, C<sub>3</sub>H<sub>8</sub> concentrations) in biosolids autocatalytic and noncatalytic pyrolysis studies as well as in mechanistic studies using bio-oil and simulated biochar catalysts was determined by gas chromatography (GC) (Agilent Technologies 7890A) with a thermal conductivity detector as described elsewhere.<sup>18</sup> Py-gas composition (H<sub>2</sub>, CH<sub>4</sub>, CO, and CO<sub>2</sub> concentrations) in mechanistic studies using simulated py-gas as feedstock was analyzed by micro-GC with a thermal conductivity detector (Agilent Technologies 490).<sup>61</sup> Other gases that could be relevant for air permitting purposes, such as NH<sub>3</sub>, NO<sub>x</sub>, and SO<sub>x</sub>, were not measured but could be significant.<sup>62</sup> The py-gas higher heating value (HHV) was calculated based on the constituent fraction and the corresponding constituent HHV. The HHVs of biochar and bio-oil were measured using a bomb calorimeter (Parr 1341, Plain Jacket Calorimeter, Parr Instrument Company, Moline, IL). The product energy per mass of biosolids pyrolyzed (kJ/kg biosolids) was calculated by multiplying each product yield with the corresponding HHV. Chemical constituents in the bio-oil were characterized by GC (7890B, Agilent Technologies, USA) mass spectroscopy (MS) (5977A, Agilent Technologies, USA) for qualitative analysis and by 430 GC/FID (Bruker Corporation, Bruker Daltonics, Inc., USA) for quantitative analysis at Iowa State University's Bioeconomy Institute as described by Brown et al.<sup>63</sup> Quantification of compounds by GC-FID was conducted using standard curves for each analyte as described previously.<sup>64</sup>

## Results and Discussion

### Impact of Autocatalytic Pyrolysis on Mass Yields and Product Composition

Using WB-biochar catalyst increased py-gas production and decreased bio-oil production ([Figure 2a](#)). The bio-oil yield decreased by 44%, changing from 36% (wt % of the total product mass) in the OB control test to approximately 20% at temperatures  $\geq 700$  °C in the autocatalytic pyrolysis tests at a catalyst/biosolids mass ratio of 1; the bio-oil yield decrease was significant at  $\geq 700$  °C (*t*test,  $p < 0.05$ ). Additional cracking (i.e., decomposition) of bio-oil by the catalyst resulted in higher py-gas yields; the py-gas yield reached its highest value of 37% at 800 °C. During the OS control test, py-gas yield increased 3.5% and 6.2% at 700 and 800 °C, respectively, when compared to the OB control. Therefore, WB-biochar autocatalytic pyrolysis resulted in py-gas yield increases greater than those of OS tests with

secondary reactions alone. Both pyrolysis reaction temperature and autocatalytic reaction temperature impact product yields. Increasing pyrolysis temperature causes an increase in py-gas yield and a slight decrease in bio-oil and biochar yield (see “0B” samples for 500 and 800 °C in [Figure 2](#)). In comparison, increasing autocatalytic temperature causes a more substantial increase in py-gas yield and a substantial decrease in bio-oil yield (see “1” samples for 500 and 800 °C in [Figure 2](#)).

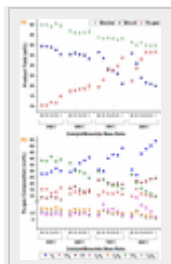


Figure 2. Autocatalytic pyrolysis impacts mass yields and shifts py-gas composition. The effect of temperature and catalyst loading on the product mass yield is shown in panel (a), and the effect on py-gas composition is shown in panel (b). The catalyst/biosolids mass ratio is noted on the x-axis. 0B denotes experiments without catalyst or sand at 500 °C; 0S denotes experiments with sand in place of catalyst. Error bars represent one standard deviation of triplicate experiments; some error bars are small and not visible. Product yields, including coke yield, are listed in [Table S2](#). The temperatures indicated were used to produce the biochar as well as perform the corresponding autocatalytic pyrolysis experiments.

Others observed py-gas yield increases when using pinewood as the feedstock and pinewood biochar as the catalyst.<sup>44,50</sup> At 500 and 600 °C, the impact of autocatalytic pyrolysis was minimal. When the catalyst/biosolids mass ratio was increased from 0.2 to 1, the bio-oil yield decreased less than 5%. Moreover, coke was formed at 700 and 800 °C ([Table S2](#)). The coke mass yield was always less than 4%.

In addition to altering mass yields, autocatalytic pyrolysis also altered py-gas composition ([Figure 2b](#)). The 0B sample represents the py-gas composition without catalyst, and the 0S sample represents the py-gas composition without catalyst but with secondary reactions. As catalyst loading increased, the H<sub>2</sub> concentration increased from approximately 30% (by volume) to 55% at 800 °C, and CO<sub>2</sub> decreased simultaneously from over 25% to 10%. The H<sub>2</sub> increase was likely a result of multiple thermochemical reactions including steam methane reforming ( $\text{H}_2\text{O} + \text{CH}_4 \leftrightarrow 3\text{H}_2 + \text{CO}$ ;  $2\text{H}_2\text{O} + \text{CH}_4 \leftrightarrow 4\text{H}_2 + \text{CO}_2$ ), dry reforming ( $\text{CO}_2 + \text{CH}_4 \leftrightarrow 2\text{CO} + 2\text{H}_2$ ), water–gas shift reaction ( $\text{CO} + \text{H}_2\text{O} \leftrightarrow \text{CO}_2 + \text{H}_2$ ), and bio-oil decomposition and reforming (e.g.,  $\text{Tar} + \text{H}_2\text{O} \rightarrow \text{CO}, \text{CO}_2, \text{and H}_2$ ). Tar decomposition to light molecular weight hydrocarbons and the H<sub>2</sub> concentration increase were ostensibly catalyzed by metals in the WB-biochar as discussed below. The CO<sub>2</sub> percentage decrease was ostensibly due to both the relative increase in H<sub>2</sub> and the dry reforming enhanced by biochar catalysts described by others.<sup>51,65,66</sup> CO may have been reduced via the water–gas shift reaction, but steam methane reforming and tar steam reforming could make up CO in addition to dry reforming. Though CH<sub>4</sub> is consumed in reforming

reactions, thermal cracking and steam reforming of tars may have compensated for the CH<sub>4</sub> decreases. CH<sub>4</sub>, C<sub>2</sub>H<sub>4</sub>, and C<sub>3</sub>H<sub>8</sub> were not major gases by concentration, but they still carried high energy values. The concentrations of C<sub>2</sub>H<sub>4</sub> and C<sub>3</sub>H<sub>8</sub> increased at 700 and 800 °C. These gases were likely produced by thermal cracking of tar at higher temperatures.<sup>67</sup>

Autocatalytic pyrolysis also altered the bio-oil chemical composition (SI, Tables S3 and S4). Based on GC-FID analysis, the 800 °C catalytic bio-oil contained few detectable organic constituents: only 3,4-dimethoxyacetophenone, 1,2,4-trimethoxybenzene, and 4-ethoxystyrene (Table S3). In contrast, 40 organic constituents were detected and quantified in the noncatalyzed 0B bio-oil by GC-FID. Also, major hydrocarbon peaks in the noncatalyzed 0B bio-oil were detected by GC-MS analysis including toluene, ethylbenzene, styrene, phenol, cresol, indole, and hydantoin (Figure S2). These peaks were not present in the 800 °C catalytic bio-oil. A detailed list of chemicals detected by GC-MS is presented in Table S4.

Along with changing the bio-oil chemical composition, autocatalytic pyrolysis substantially changed the bio-oil color (Figure S3). The aqueous layer in the catalytic bio-oil was translucent compared to noncatalytic bio-oil that was brown. In addition to the color, light nonaqueous phase liquid volume was greatly reduced. Very little light nonaqueous phase liquid was observed in the bio-oil catalyzed at 700 °C, and none was observed at 800° (Figure S3). Dark bio-oil color is associated with the presence of unsaturated hydrocarbons.<sup>68</sup> Therefore, autocatalytic pyrolysis led to fewer unsaturated hydrocarbons in the bio-oil, which could be advantageous during subsequent upgrading or disposal. Future work is warranted to determine the complete chemical composition of catalyzed and other bio-oils.

#### Impact of Autocatalytic Pyrolysis on Py-Gas and Bio-Oil Energy Yields

Autocatalytic pyrolysis reduced the bio-oil energy content (Figure S4), and the bio-oil HHV decreased with increased catalyst/biosolids mass ratios at each pyrolysis temperature. In particular, at 800 °C, the bio-oil HHV decreased from 8070 kJ/kg-bio-oil with no catalysis (0B) to below 1400 kJ/kg-bio-oil at the highest catalyst loading ratio of 1:1. The HHV decrease was likely due to the decrease in organic constituents described above and the formation of water during catalysis.<sup>51</sup> The py-gas HHV during 0S pyrolysis conditions increased greatly at higher temperatures of 700 and 800 °C due to increased concentrations of CH<sub>4</sub>, C<sub>2</sub>H<sub>4</sub>, and C<sub>3</sub>H<sub>8</sub>, which have high unit energy contents. However, when more H<sub>2</sub> (comparatively lower volumetric energy content) was produced via autocatalytic pyrolysis, the py-gas HHV decreased.

Energy yields associated with py-gas increased as temperature and catalyst/biosolids mass ratio increased (Figure 3). For the noncatalyzed 0B control tests, more energy was produced in the form of bio-oil than py-gas at 500 and 600 °C; at temperatures of 700 and 800 °C, the energies in bio-oil and py-gas were approximately equal.

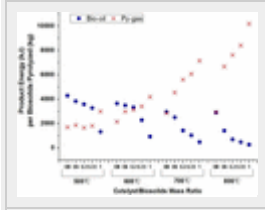


Figure 3. Autocatalytic pyrolysis affects py-gas and bio-oil energy yields. OB denotes experiments without catalyst or sand at 500 °C; OS denotes experiments with sand in place of catalyst.

Secondary reactions under noncatalyzed OS conditions shifted some energy from bio-oil to py-gas. The addition of WB-biochar catalyst further increased py-gas energy yield. At the highest catalyst loading, the py-gas energy increased to 10,200 kJ/kg-biosolids-pyrolyzed from the original 2940 kJ/kg-biosolids-pyrolyzed under noncatalyzed OB condition at 800 °C. Meanwhile, due to the greatly reduced yield and energy content in bio-oil, the bio-oil energy decreased from 2900 kJ/kg-biosolids-pyrolyzed to 275 kJ/kg-biosolids-pyrolyzed. The shift from bio-oil to py-gas energy may be especially useful for utilities that already combust anaerobic digester biogas for on-site energy recovery; it may be possible to blend biogas and py-gas for combined use.

#### Mechanistic Studies Using Bio-Oil or Simulated Py-Gas Alone

Bio-oil fed to the reactor vessel alone decomposed when WB-biochar was employed as a catalyst. The bio-oil mass decreased by 40% (from 10 to 6 g) during the mechanistic studies using bio-oil; this decrease was similar to the bio-oil reduction during autocatalytic pyrolysis of biosolids at 800 °C with a catalyst/biosolids mass ratio of 0.33 (i.e., from 36% to 22%). In addition, the bio-oil fed alone produced H<sub>2</sub>, CH<sub>4</sub>, CO, CO<sub>2</sub>, and C<sub>2</sub>H<sub>4</sub>, in which H<sub>2</sub> had the highest percentage of 63% (Figure 4). These results demonstrate that the WB-biochar catalyst converted bio-oil into py-gas and corroborates results shown in Figure 2; destruction and reforming of bio-oil by WB-biochar catalyst was a significant contributor to the H<sub>2</sub> increase.

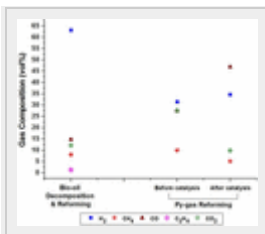


Figure 4. Py-gas composition during autocatalytic decomposition and reforming of bio-oil alone (left and reforming of py-gas (right)). Error bars represent one standard deviation of triplicate experiments; some error bars are small and not visible.

Simulated py-gas fed to the reactor vessel alone was also reformed via autocatalytic pyrolysis. CO increased from 27% to 47%, while CO<sub>2</sub> decreased from 27% to 10% (Figure 4). The CH<sub>4</sub> content was also reduced by 50% when the catalyst was present. However, H<sub>2</sub> concentration only increased slightly.

#### Autocatalytic Role of Dominant Metals in WB-Biochar

Metals present in WB-biochar were responsible for a majority of the catalytic activity. The addition of Ca and Fe significantly influenced both product distribution and py-gas composition (Figure 5). The Ca<sup>2+</sup> and Fe<sup>3+</sup> reduced bio-oil yield from over 35% (OB) to 25% and increased the py-gas yield from 22% (OB) to 34%. The H<sub>2</sub> concentration increased from 31% (OB) to 37% when Ca<sup>2+</sup> and Fe<sup>3+</sup> were present in biochar. The metal oxides catalytic effects were similar to those of metal salts. The presence of CaO and Fe<sub>2</sub>O<sub>3</sub> in biochar increased the H<sub>2</sub> concentration to 40% and decreased bio-oil yield to approximately 24%, while py-gas yield increased to 35% (Figure 5). The concentrations of other py-gas constituents produced using WB-biochar and simulated catalysts were similar (Figures 2b and 5b). Previous research demonstrated that Mg<sup>2+</sup> and MgO in catalysts reduced tar or bio-oil production.<sup>55, 58</sup> The low Mg<sup>2+</sup> content in these simulated catalyst experiments were based on the Mg<sup>2+</sup> content in the feed biosolids and did not change the product yields (Mg<sup>2+</sup> data are not shown).

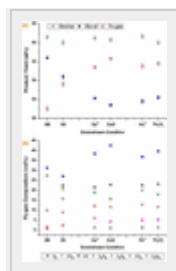


Figure 5. Catalytic effect of metals on product yields (a) and py-gas composition (b). OB denotes experiments without catalyst or sand at 500 °C; OS denotes experiments with sand in place of catalyst. Error bars represent one standard deviation of triplicate experiments.

WB-biochar and the metals it contains may facilitate bio-oil decomposition by absorption-enhanced reforming.<sup>60,69</sup> Others have shown that tar constituents readily adsorb onto char and metal surfaces and then dissociate to reactive radicals such as aromatic ring fragments.<sup>47,60,69-72</sup> WB-biochar itself also contains free radicals in the carbon matrix that are generated by decomposition of organic matter during pyrolysis and subsequent cooling in air.<sup>73-75</sup> The porous carbon structure and the highly dispersed metals likely act as active sites for radical reactions, converting tar constituents to smaller molecules and gases.<sup>47,76-78</sup> In particular, high temperature favors free-radical reactions.<sup>79</sup> Also, iron oxides are the major component of commercial catalysts for high-temperature water–gas shift reaction.<sup>80,81</sup> The py-gas H<sub>2</sub> concentration increase observed may have resulted from the catalytic water–gas shift reaction. Moreover, iron oxides or ions could be partially transformed into metallic states via *in situ* reduction by carbon (i.e., the char part of WB-biochar) or reductive gases (e.g., H<sub>2</sub> and CO) from biosolids pyrolysis.<sup>82-84</sup> The metallic irons could also enhance tar decomposition.<sup>57,85</sup>

Additionally, CaO can play a role in increased H<sub>2</sub> production by *in situ* removal of CO<sub>2</sub> from the py-gas.<sup>86</sup> In this sorption-enhanced hydrogen production process, there are many CO<sub>2</sub>-producing reactions that can be involved such as steam methane reforming and water–gas shift reaction.<sup>87,88</sup>

In summary, using biochar produced from wastewater biosolids as a catalyst can significantly alter the products derived from pyrolysis of the same wastewater biosolids. The autocatalytic pyrolysis process yielded more py-gas that is relatively clean and easily combusted for energy in existing boilers or engines, less bio-oil requiring conditioning or disposal, and biochar that is a valuable soil amendment. This work is the first research to demonstrate the autocatalytic effect of WB-biochar on product distribution and energy recovery during biosolids pyrolysis. The autocatalytic pyrolysis process could be a step to enhance energy recovery, minimize adverse environmental impacts, and generate value-added products from used water. The shift from bio-oil to py-gas energy may be useful at WRRFs that already combust anaerobic digester biogas for on-site energy recovery; it may be possible to blend biogas and py-gas for combined use.

The authors declare no competing financial interest.

## Acknowledgment

Funding for this work was provided by the Milwaukee Metropolitan Sewerage District, Water Quality Center at Marquette University, and Marquette University. Laboratory assistance from John Kissel, Mark Wendtland, Hui Liu, Erik Anderson, and Matthew Hughes is greatly appreciated. We are also grateful to Dr. Robert Brown and Mr. Patrick Johnston of the Iowa State University Bioeconomy Institute for providing GC-MS and GC-FID bio-oil analyses. GC-MS and GC-FID bio-oil analysis as well as Dr. Jier Huang in the Chemistry Department at Marquette University for use of her micro-GC.

## References

- <sup>1</sup>Jhansi, S. C.; Mishra, S. K. Wastewater Treatment and Reuse: Sustainability Options *Cons. J. Sustain. Dev.* **2013**, 10 (1) 1– 15
- <sup>2</sup>Eggen, R. I. L.; Hollender, J.; Joss, A.; Schärer, M.; Stamm, C. Reducing the discharge of micropollutants in the aquatic environment: the benefits of upgrading wastewater treatment plants *Environ. Sci. Technol.* **2014**, 48 (14) 7683– 7689 DOI: 10.1021/es500907n
- <sup>3</sup>Venkatesan, A. K.; Hamdan, A.-H. M.; Chavez, V. M.; Brown, J. D.; Halden, R. U. Mass Balance Model for Sustainable Phosphorus Recovery in a US Wastewater Treatment Plant *J. Environ. Qual.* **2016**, 45 (1) 84–89 DOI: 10.2134/jeq2014.11.0504
- <sup>4</sup>Mo, W.; Zhang, Q. Energy-nutrients-water nexus: integrated resource recovery in municipal wastewater treatment plants *J. Environ. Manage.* **2013**, 127, 255– 267 DOI: 10.1016/j.jenvman.2013.05.007
- <sup>5</sup>Gude, V. Energy positive wastewater treatment and sludge management *Edorium J. Waste Management* **2015**, 1, 10– 15

- <sup>6</sup>Cao, Y.; Pawłowski, A. Sewage sludge-to-energy approaches based on anaerobic digestion and pyrolysis: Brief overview and energy efficiency assessment *Renewable Sustainable Energy Rev.* **2012**, 16 (3) 1657–1665 DOI: 10.1016/j.rser.2011.12.014
- <sup>7</sup>Xia, K.; Hundal, L.; Kumar, K. Triclocarban, triclosan, polybrominated diphenyl ethers, and 4-nonylphenol in biosolids and in soil receiving 33-year biosolids application *Environ. Toxicol. Chem.* **2010**, 29(3) 597– 605 DOI: 10.1002/etc.66
- <sup>8</sup>Bright, D. A.; Healey, N. Contaminant risks from biosolids land application *Environ. Pollut.* **2003**, 126 (1) 39–49 DOI: 10.1016/S0269-7491(03)00148-9
- <sup>9</sup>Singh, R. P.; Agrawal, M. Potential benefits and risks of land application of sewage sludge *Waste Manage.* **2008**, 28 (2) 347– 358 DOI: 10.1016/j.wasman.2006.12.010
- <sup>10</sup>Carey, D. E.; Zitomer, D. H.; Hristova, K. R.; Kappell, A. D.; McNamara, P. J. Triclocarban Influences Antibiotic Resistance and Alters Anaerobic Digester Microbial Community Structure *Environ. Sci. Technol.* **2016**, 50 (1) 126– 134 DOI: 10.1021/acs.est.5b03080
- <sup>11</sup>Carey, D.; Zitomer, D. H.; Kappell, A.; Choi, M.; Hristova, K. H.; McNamara, P. Chronic exposure to triclosan sustains microbial community shifts and alters antibiotic resistance gene levels in anaerobic digesters *Environ. Sci. Process. Impacts* **2016**, 18 (8) 1060– 1067 DOI: 10.1039/C6EM00282J
- <sup>12</sup>Torri, S.; Corrêa, R. Biosolids soil application: why a new special on an old issue? *Appl. Environ. Soil Sci.* **2012**, 2012, 1– 3 DOI: 10.1155/2012/145724
- <sup>13</sup>Evans, T. D. Biosolids in Europe *Proc. Water Environ. Fed.* **2012**, 2012 (2) 108– 117 DOI: 10.2175/193864712811694253
- <sup>14</sup>Rulkens, W. Sewage sludge as a biomass resource for the production of energy: Overview and assessment of the various options *Energy Fuels* **2008**, 22 (1) 9– 15 DOI: 10.1021/ef700267m
- <sup>15</sup>Chen, D.; Yu, Y.; Zhu, H.; Liu, Z.; Xu, Y. Ferrite process of electroplating sludge and enrichment of copper by hydrothermal reaction *Sep. Purif. Technol.* **2008**, 62 (2) 297– 303 DOI: 10.1016/j.seppur.2008.01.003
- <sup>16</sup>Lumley, N. P. G.; Ramey, D. F.; Prieto, A. L.; Braun, R. J.; Cath, T. Y.; Porter, J. M. Techno-economic analysis of wastewater sludge gasification: A decentralized urban perspective *Bioresour. Technol.* **2014**, 161, 385– 394 DOI: 10.1016/j.biortech.2014.03.040
- <sup>17</sup>Bridle, T.; Pritchard, D. Energy and nutrient recovery from sewage sludge via pyrolysis *Water Sci. Technol.* **2004**, 50 (9) 169– 175
- <sup>18</sup>McNamara, P.; Koch, J.; Zitomer, D. Pyrolysis of Wastewater Biosolids: Lab-Scale Experiments and Modeling *Proc. Water Environ. Fed.* **2014**, 2014 (2) 1– 14 DOI: 10.2175/193864714816196655
- <sup>19</sup>Liu, Z.; Qian, G.; Sun, Y.; Xu, R.; Zhou, J.; Xu, Y. Speciation Evolutions of Heavy Metals during the Sewage Sludge Incineration in a Laboratory Scale Incinerator *Energy Fuels* **2010**, 24 (4) 2470– 2478 DOI: 10.1021/ef901060u

- <sup>20</sup>Fytilli, D.; Zabaniotou, A. Utilization of sewage sludge in EU application of old and new methods—A review *Renewable Sustainable Energy Rev.* **2008**, 12 (1) 116– 140 DOI: 10.1016/j.rser.2006.05.014
- <sup>21</sup>Liu, Z. Development of a Sorption Enhanced Steam Hydrogasification Process for in-Situ Carbon Dioxide (CO<sub>2</sub>) Removal and Enhanced Synthetic Fuel Production. Ph.D. Thesis, University of California, Riverside, **2014**.
- <sup>22</sup>Samolada, M. C.; Zabaniotou, A. A. Comparative assessment of municipal sewage sludge incineration, gasification and pyrolysis for a sustainable sludge-to-energy management in Greece *Waste Manage.* **2014**, 34 (2) 411– 420 DOI: 10.1016/j.wasman.2013.11.003
- <sup>23</sup>Carey, D. E.; McNamara, P. J.; Zitomer, D. H. Biochar from Pyrolysis of Biosolids for Nutrient Adsorption and Turfgrass Cultivation *Water Environ. Res.* **2015**, 87 (12) 2098– 2106 DOI: 10.2175/106143015X14362865227391
- <sup>24</sup>Ross, J. J.; Zitomer, D. H.; Miller, T. R.; Weirich, C. A.; McNamara, P. J. Emerging investigators series: pyrolysis removes common microconstituents triclocarban, triclosan, and nonylphenol from biosolids *Environ. Sci. Water Res. Technol.* **2016**, 2 (2) 282– 289 DOI: 10.1039/C5EW00229J
- <sup>25</sup>Hoffman, T. C.; Zitomer, D. H.; McNamara, P. J. Pyrolysis of Wastewater Biosolids Significantly Reduces Estrogenicity *J. Hazard. Mater.* **2016**, 317, 579– 584 DOI: 10.1016/j.jhazmat.2016.05.088
- <sup>26</sup>McNamara, P.; Koch, J.; Liu, Z.; Zitomer, D. H. Pyrolysis of dried wastewater biosolids can be energy positive *Water Environ. Res.* **2016**, 88 (9) 804– 810 DOI: 10.2175/106143016X14609975747441
- <sup>27</sup>Lu, H.; Zhang, W.; Wang, S.; Zhuang, L. Characterization of sewage sludge-derived biochars from different feedstocks and pyrolysis temperatures *J. Anal. Appl. Pyrolysis* **2013**, 102, 137– 143 DOI: 10.1016/j.jaap.2013.03.004
- <sup>28</sup>Xu, W.; Wu, D. Comprehensive utilization of the pyrolysis products from sewage sludge *Environ. Technol.* **2015**, 36 (14) 1731– 1744 DOI: 10.1080/09593330.2015.1008584
- <sup>29</sup>Khanmohammadi, Z. Effect of pyrolysis temperature on chemical and physical properties of sewage sludge biochar *Waste Manage. Res.* **2015**, 33 (3) 275– 283 DOI: 10.1177/0734242X14565210
- <sup>30</sup>Conesa, J.; Marcilla, A.; Moral, R. Evolution of gases in the primary pyrolysis of different sewage sludges *Thermochim. Acta* **1998**, 313 (1) 63– 73 DOI: 10.1016/S0040-6031(97)00474-7
- <sup>31</sup>Yuan, H.; Lu, T.; Zhao, D.; Huang, H. Influence of temperature on product distribution and biochar properties by municipal sludge pyrolysis *J. Mater. Cycles Waste Manage.* **2013**, 15 (3) 357– 361 DOI: 10.1007/s10163-013-0126-9
- <sup>32</sup>Inguanzo, M.; Dominguez, A. On the pyrolysis of sewage sludge: the influence of pyrolysis conditions on solid, liquid and gas fractions *J. Anal. Appl. Pyrolysis* **2002**, 63 (1) 209– 222 DOI: 10.1016/S0165-2370(01)00155-3
- <sup>33</sup>Thipkhunthod, P.; Meeyoo, V. Pyrolytic characteristics of sewage sludge *Chemosphere* **2006**, 64 (6) 955– 962 DOI: 10.1016/j.chemosphere.2006.01.002



- <sup>34</sup>Fonts, I.; Gea, G.; Azuara, M.; Ábrego, J.; Arauzo, J. Sewage sludge pyrolysis for liquid production: A review *Renewable Sustainable Energy Rev.* **2012**, 16 (5) 2781– 2805 DOI: 10.1016/j.rser.2012.02.070
- <sup>35</sup>Lu, G.; Low, J.; Liu, C.; Lua, A. Surface area development of sewage sludge during pyrolysis *Fuel* **1995**, 74(3) 344– 348 DOI: 10.1016/0016-2361(95)93465-P
- <sup>36</sup>Hossain, M.; Strezov, V.; Nelson, P. Thermal characterisation of the products of wastewater sludge pyrolysis *J. Anal. Appl. Pyrolysis* **2009**, 85 (1) 442– 446 DOI: 10.1016/j.jaap.2008.09.010
- <sup>37</sup>Baratieri, M.; Baggio, P.; Bosio, B.; Grigante, M.; Longo, G. A. The use of biomass syngas in IC engines and CCGT plants: A comparative analysis *Appl. Therm. Eng.* **2009**, 29 (16) 3309– 3318 DOI: 10.1016/j.applthermaleng.2009.05.003
- <sup>38</sup>Lehto, J.; Oasmaa, A.; Solantausta, Y. Fuel oil quality and combustion of fast pyrolysis bio-oils. *VTT Technol.* **2013**.
- <sup>39</sup>Oasmaa, A.; Czernik, S. Fuel oil quality of biomass pyrolysis oils state of the art for the end users *Energy Fuels* **1999**, 13 (4) 914– 921 DOI: 10.1021/ef980272b
- <sup>40</sup>Sadaka, S.; Boateng, A. *Pyrolysis and Bio-Oil*; University of Arkansas, **2009**.
- <sup>41</sup>Vreugdenhil, B.; Zwart, R.; Neeft, J. *Tar Formation in Pyrolysis and Gasification*; Energy Research Centre of the Netherlands, **2009**.
- <sup>42</sup>Daintith, J. *A Dictionary of Chemistry*; Oxford University Press, **2008**.
- <sup>43</sup>Zhang, Y. L.; Luo, Y. H.; Wu, W. G.; Zhao, S. H.; Long, Y. F. Heterogeneous cracking reaction of tar over biomass char, using naphthalene as model biomass tar *Energy Fuels* **2014**, 28 (5) 3129– 3137 DOI: 10.1021/ef4024349
- <sup>44</sup>Sun, Q.; Yu, S.; Wang, F.; Wang, J. Decomposition and gasification of pyrolysis volatiles from pine wood through a bed of hot char *Fuel* **2011**, 90 (3) 1041– 1048 DOI: 10.1016/j.fuel.2010.12.015
- <sup>45</sup>Klinghoffer, N. B.; Castaldi, M. J.; Nzihou, A. Catalyst properties and catalytic performance of char from biomass gasification *Ind. Eng. Chem. Res.* **2012**, 51 (40) 13113– 13122 DOI: 10.1021/ie3014082
- <sup>46</sup>Wang, F. J.; Zhang, S.; Chen, Z. D.; Liu, C.; Wang, Y. G. Tar reforming using char as catalyst during pyrolysis and gasification of Shengli brown coal *J. Anal. Appl. Pyrolysis* **2014**, 105, 269– 275 DOI: 10.1016/j.jaap.2013.11.013
- <sup>47</sup>Min, Z.; Yimsiri, P.; Asadullah, M.; Zhang, S.; Li, C. Catalytic reforming of tar during gasification. Part II. Char as a catalyst or as a catalyst support for tar reforming *Fuel* **2011**, 90 (7) 2545– 2552 DOI: 10.1016/j.fuel.2011.03.027
- <sup>48</sup>Abu El-Rub, Z.; Bramer, E. A.; Brem, G. Experimental comparison of biomass chars with other catalysts for tar reduction *Fuel* **2008**, 87 (10–11) 2243– 2252 DOI: 10.1016/j.fuel.2008.01.004
- <sup>49</sup>Mani, S.; Kastner, J. R.; Juneja, A. Catalytic decomposition of toluene using a biomass derived catalyst *Fuel Process. Technol.* **2013**, 114, 118– 125 DOI: 10.1016/j.fuproc.2013.03.015

- <sup>50</sup>Gilbert, P.; Ryu, C.; Sharifi, V.; Swithenbank, J. Tar reduction in pyrolysis vapours from biomass over a hot char bed *Bioresour. Technol.* **2009**, 100 (23) 6045– 6051 DOI: 10.1016/j.biortech.2009.06.041
- <sup>54</sup>Ren, S.; Lei, H.; Wang, L.; Bu, Q.; Chen, S.; Wu, J. Hydrocarbon and hydrogen-rich syngas production by biomass catalytic pyrolysis and bio-oil upgrading over biochar catalysts *RSC Adv.* **2014**, 4 (21) 10731–10737 DOI: 10.1039/C4RA00122B
- <sup>52</sup>ASTM D7582-15 Standard Test Methods for Proximate Analysis of Coal and Coke by Macro Thermogravimetric Analysis. <https://www.astm.org/Standards/D7582.htm> (accessed June 6, **2017**) .
- <sup>53</sup>Ahuja, P.; Kumar, S.; Singh, P. C. A model for primary and heterogeneous secondary reactions of wood pyrolysis *Chem. Eng. Technol.* **1996**, 19 (3) 272– 282 DOI: 10.1002/ceat.270190312
- <sup>54</sup>Porosity Measurement, <http://infohost.nmt.edu/~petro/faculty/Engler524/PET524-porosity-2-ppt.pdf>. (accessed June 5, **2017**) .
- <sup>55</sup>El-Rub, Z. A.; Bramer, E.; Brem, G. Review of catalysts for tar elimination in biomass gasification processes *Ind. Eng. Chem. Res.* **2004**, 43 (22) 6911– 6919 DOI: 10.1021/ie0498403
- <sup>56</sup>Min, Z.; Asadullah, M.; Yimsiri, P.; Zhang, S.; Wu, H.; Li, C. Z. Catalytic reforming of tar during gasification. Part I. Steam reforming of biomass tar using ilmenite as a catalyst *Fuel* **2011**, 90 (5) 1847– 1854 DOI: 10.1016/j.fuel.2010.12.039
- <sup>57</sup>Nordgreen, T.; Liliedahl, T.; Sjöström, K. Metallic iron as a tar breakdown catalyst related to atmospheric, fluidised bed gasification of biomass *Fuel* **2006**, 85 (5) 689– 694 DOI: 10.1016/j.fuel.2005.08.026
- <sup>58</sup>Liu, H.; Ma, X.; Li, L.; Hu, Z.; Guo, P.; Jiang, Y. The catalytic pyrolysis of food waste by microwave heating *Bioresour. Technol.* **2014**, 166, 45– 50 DOI: 10.1016/j.biortech.2014.05.020
- <sup>59</sup>Hayashi, J.; Iwatsuki, M.; Morishita, K.; Tsutsumi, A. Roles of inherent metallic species in secondary reactions of tar and char during rapid pyrolysis of brown coals in a drop-tube reactor *Fuel* **2002**, 81 (15)1977– 1987 DOI: 10.1016/S0016-2361(02)00128-X
- <sup>60</sup>Uddin, M.; Tsuda, H.; Wu, S.; Sasaoka, E. Catalytic decomposition of biomass tars with iron oxide catalysts *Fuel* **2008**, 87 (4-5) 451– 459 DOI: 10.1016/j.fuel.2007.06.021
- <sup>61</sup>Yang, S.; Pattengale, B.; Kovrigin, E.; Huang, J. Photoactive Zeolitic Imidazolate Framework as Intrinsic Heterogeneous Catalysts for Light-Driven Hydrogen Generation *ACS Energy Lett.* **2017**, 2 (1) 75– 80 DOI: 10.1021/acsenergylett.6b00540
- <sup>62</sup>Tian, Y.; Zhang, J.; Zuo, W.; Chen, L.; Cui, Y.; Tan, T. Nitrogen Conversion in Relation to NH<sub>3</sub> and HCN during Microwave Pyrolysis of Sewage Sludge *Environ. Sci. Technol.* **2013**, 47 (7) 3498– 3505 DOI: 10.1021/es304248j
- <sup>63</sup>Rover, M.; Hall, P.; Johnston, P.; Smith, R.; Brown, R. Stabilization of bio-oils using low temperature, low pressure hydrogenation *Fuel* **2015**, 153, 224– 230 DOI: 10.1016/j.fuel.2015.02.054

- <sup>64</sup>Choi, Y. S.; Johnston, P. A.; Brown, R. C.; Shanks, B. H.; Lee, K. H. Detailed characterization of red oak-derived pyrolysis oil: Integrated use of GC, HPLC, IC, GPC and Karl-Fischer *J. Anal. Appl. Pyrolysis* **2014**, 110, 147– 154 DOI: 10.1016/j.jaap.2014.08.016
- <sup>65</sup>Muradov, N.; Fidalgo, B.; Gujar, A. C.; Garceau, N.; T-Raissi, A. Production and characterization of Lemna minor bio-char and its catalytic application for biogas reforming *Biomass Bioenergy* **2012**, 42, 123– 131 DOI: 10.1016/j.biombioe.2012.03.003
- <sup>66</sup>Domínguez, A.; Fernández, Y.; Fidalgo, B.; Pis, J. J.; Menéndez, J. A. Biogas to Syngas by Microwave-Assisted Dry Reforming in the Presence of Char *Energy Fuels* **2007**, 21 (4) 2066– 2071 DOI: 10.1021/ef070101j
- <sup>67</sup>Namioka, T.; Son, Y.; Sato, M.; Yoshikawa, K. Practical method of gravimetric tar analysis that takes into account a thermal cracking reaction scheme *Energy Fuels* **2009**, 23 (12) 6156– 6162 DOI: 10.1021/ef9006214
- <sup>68</sup>Sappok, M.; Wagels, D. Method for stabilizing heating oil or diesel oil, particularly heating oil or diesel oil from the depolymerization of hydrocarbon-containing residues, or pyrolysis oil. U.S. Patent 8,394,264, **2013**.
- <sup>69</sup>Polychronopoulou, K.; Bakandritsos, A.; Tzitzios, V.; Fierro, J.; Efstathiou, A. Absorption-enhanced reforming of phenol by steam over supported Fe catalysts *J. Catal.* **2006**, 241 (1) 132– 148 DOI: 10.1016/j.jcat.2006.04.015
- <sup>70</sup>Shen, Y.; Yoshikawa, K. Recent progresses in catalytic tar elimination during biomass gasification or pyrolysis-A review *Renewable Sustainable Energy Rev.* **2013**, 21, 371– 392 DOI: 10.1016/j.rser.2012.12.062
- <sup>71</sup>Aldén, H.; Björkman, E., et al. Catalytic Cracking of Naphthalene on Dolomite. In *Advances in Thermochemical Biomass Conversion*; Springer, **1993**; pp 216– 232.
- <sup>72</sup>Taralas, G.; Vassilatos, V.; Sjöström, K.; Delgado, J. Thermal and catalytic cracking of n -Heptane in presence of CaO, MgO and Calcined Dolomites *Can. J. Chem. Eng.* **1991**, 69 (6) 1413– 1419 DOI: 10.1002/cjce.5450690626
- <sup>73</sup>Amonette, J.; Joseph, S. Characteristics of Biochar: Microchemical Properties. In *Biochar for Environmental Management: Science and Technology*; Earthscan, **2009**; pp 33– 51.
- <sup>74</sup>Liao, S.; Pan, B.; Li, H.; Zhang, D.; Xing, B. Detecting free radicals in biochars and determining their ability to inhibit the germination and growth of corn, wheat and rice seedlings *Environ. Sci. Technol.* **2014**, 48 (15)8581– 8587 DOI: 10.1021/es404250a
- <sup>75</sup>Pignatello, J. J.; Mitch, W. A.; Xu, W. Activity and reactivity of pyrogenic carbonaceous matter toward organic compounds *Environ. Sci. Technol.* **2017**, 51 (16) 8893– 8908 DOI: 10.1021/acs.est.7b01088
- <sup>76</sup>Li, C. Importance of volatile-char interactions during the pyrolysis and gasification of low-rank fuels—a review *Fuel* **2013**, 112, 609– 623 DOI: 10.1016/j.fuel.2013.01.031
- <sup>77</sup>Weston, P. M.; Sharifi, V.; Swithenbank, J. Destruction of Tar in a Novel Coandă Tar Cracking System *Energy Fuels* **2014**, 28 (2) 1059– 1065 DOI: 10.1021/ef401705g

- <sup>78</sup>Zhang, S.; Asadullah, M.; Dong, L.; Tay, H.; Li, C. An advanced biomass gasification technology with integrated catalytic hot gas cleaning. Part II: Tar reforming using char as a catalyst or as a catalyst support *Fuel* **2013**, 112, 646– 653 DOI: 10.1016/j.fuel.2013.03.015
- <sup>79</sup>Li, Y.; Guo, L.; Zhang, X.; Jin, H.; Lu, Y. Hydrogen production from coal gasification in supercritical water with a continuous flowing system *Int. J. Hydrogen Energy* **2010**, 35 (7) 3036– 3045 DOI: 10.1016/j.ijhydene.2009.07.023
- <sup>80</sup>Newsome, D. S. The Water-Gas Shift Reaction *Catal. Rev.: Sci. Eng.* **1980**, 21 (2) 275– 318 DOI: 10.1080/03602458008067535
- <sup>81</sup>Natesakhawat, S.; Wang, X.; Zhang, L.; Ozkan, U. S. Development of chromium-free iron-based catalysts for high-temperature water-gas shift reaction *J. Mol. Catal. A: Chem.* **2006**, 260 (1– 2) 82– 94 DOI: 10.1016/j.molcata.2006.07.013
- <sup>82</sup>Shen, Y.; Zhao, P.; Shao, Q.; Ma, D.; Takahashi, F.; Yoshikawa, K. In-situ catalytic conversion of tar using rice husk char-supported nickel-iron catalysts for biomass pyrolysis/gasification *Appl. Catal., B* **2014**, 152-153, 140– 151 DOI: 10.1016/j.apcatb.2014.01.032
- <sup>83</sup>Guan, G.; Chen, G.; Kasai, Y.; Lim, E. W. C.; Hao, X.; Kaewpanha, M.; Abuliti, A.; Fushimi, C.; Tsutsumi, A. Catalytic steam reforming of biomass tar over iron- or nickel-based catalyst supported on calcined scallop shell *Appl. Catal., B* **2012**, 115-116, 159– 168 DOI: 10.1016/j.apcatb.2011.12.009
- <sup>84</sup>Fruehan, R. J. The rate of reduction of iron oxides by carbon *Metall. Trans. B* **1977**, 8 (1) 279– 286 DOI: 10.1007/BF02657657
- <sup>85</sup>Nordgreen, T.; Liliedahl, T.; Sjöström, K. Elemental Iron as a Tar Breakdown Catalyst in Conjunction with Atmospheric Fluidized Bed Gasification of Biomass: A Thermodynamic Study *Energy Fuels* **2006**, 20 (3) 890– 895 DOI: 10.1021/ef0502195
- <sup>86</sup>Florin, N. H.; Harris, A. T. Enhanced hydrogen production from biomass with in situ carbon dioxide capture using calcium oxide sorbents *Chem. Eng. Sci.* **2008**, 63 (2) 287– 316 DOI: 10.1016/j.ces.2007.09.011
- <sup>87</sup>Liu, Z.; Park, C.; Norbeck, J. Sorption enhanced steam hydrogasification of coal for synthesis gas production with in-situ CO<sub>2</sub> removal and self-sustained hydrogen supply *Int. J. Hydrogen Energy* **2013**, 38(17) 7016– 7025 DOI: 10.1016/j.ijhydene.2013.03.146
- <sup>88</sup>Harrison, D. P. Sorption-Enhanced Hydrogen Production: A Review *Ind. Eng. Chem. Res.* **2008**, 47 (17) 6486– 6501 DOI: 10.1021/ie800298z

### Supporting Information

The Supporting Information is available free of charge on the [ACS Publications website](http://acs.org) at DOI: [10.1021/acs.est.7b02913](https://doi.org/10.1021/acs.est.7b02913).